

Adsorption-induced chirality influences surface orientation in organic self-assembled structures: an STM study of PVBA on Pd(1 1 1)

Byung-Il Kim¹, Chengzhi Cai, Xiaobin Deng, Scott S. Perry^{*}

Department of Chemistry, University of Houston, Houston, TX 77204-5003, USA

Received 31 October 2002; accepted for publication 24 April 2003

Abstract

The adsorption of the planar organic molecule, 4-*trans*-2-(pyrid-4-yl-vinyl) benzoic acid (PVBA), on Pd(1 1 1) under ultrahigh vacuum conditions produces molecular dimers and trimers. Scanning tunneling microscopy (STM) images reveal that dimers are formed preferentially over the trimer structures. Adsorption of the asymmetric planar molecule induces chirality in the adsorbed structures and results in homo-chiral and hetero-chiral dimers of PVBA. The STM results further reveal an orientation-specific adsorption of the different chiralities. A statistical analysis of the observed structures indicates an equivalent presence of the two dimer types on a surface not inherently offering any form of chiral recognition. The chiral dimer pairs are further resolved through site-specific adsorption orientations with respect to the Pd lattice. These investigations demonstrate the cooperative roles of substrate–adsorbate binding and intermolecular interactions in the formation of these self-assembled structures.

© 2003 Elsevier Science B.V. All rights reserved.

Keywords: Scanning tunneling microscopy; Self-assembly; Palladium; Aromatics

1. Introduction

The adsorption and/or self-assembly of organic molecules at surfaces have been extensively investigated with a wide range of techniques over the past two decades. In addition to the structural characterization of the adsorption site and geometry, many reports of self-assembled systems

have discussed the interplay between intermolecular interactions among adsorbates and substrate–adsorbate interactions and its role in determining the resulting structure. Recently, a number of studies have explored chirality in adsorbed organic species. Studies have addressed (i) enantiomeric selectivity through chiral adsorption sites [1–7], (ii) surface-induced chirality upon the adsorption of 3D molecular structures [8–13] and (iii) surface-induced chirality of 2D planar molecules [14–21]. Within the latter category, the adsorption of 4-*trans*-2-(pyrid-4-yl-vinyl) benzoic acid (PVBA) has been studied on a range of surfaces differing in both composition and structure. PVBA (Fig. 1) consists of two aromatic rings (the pyridyl group

^{*} Corresponding author. Tel.: +713-743-2715; fax: +713-743-2709.

E-mail address: perry@uh.edu (S.S. Perry).

¹ Present address: Sandia National Laboratories, Albuquerque NM.

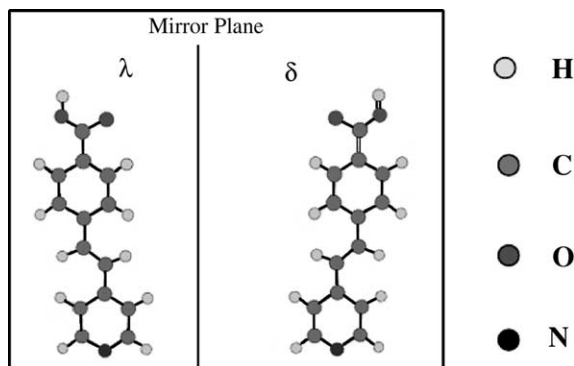


Fig. 1. The molecular structure of 4-*trans*-2-(pyrid-4-yl-vinyl) benzoic acid (PVBA) includes a pyridyl group and a benzoic acid moiety connected through a vinyl linkage. Two different adsorption geometries (“ δ ” and “ λ ”) result from a surface-induced chirality.

and benzoic acid) linked via a vinylene group and is essentially planar with an extended π -electron system [22–24]. PVBA was initially designed for nonlinear optical applications. The PVBA adsorption system is particularly interesting as crystallographic structure of the substrate, surface-induced chirality, and intermolecular hydrogen bonding interactions have all been observed to play roles in determining the resulting structure of the adsorbed/self-assembled system. Previous low coverage studies have observed the adsorption of isolated PVBA molecules on Pd(1 1 0) [17–19] and the formation of extended 2D chains of PVBA on Ag(1 1 1) and Au(1 1 1) [19–21].

In this paper, we report the results of adsorbing PVBA on a Pd(1 1 1) surface and the formation of novel dimer adsorption structures, distinguished through their surface induced chirality. Measurements have been performed with scanning tunneling microscopy (STM) at room temperature and have enabled the visualization and identification of these nano-scale structures. A comparison of the adsorption properties of PVBA on Pd(1 1 1) to those encountered for PVBA on the other surfaces highlights the delicate balance between surface and intermolecular interactions and the opportunity for further tailoring self-assembled nanostructures through molecular design.

2. Experimental

All experiments were conducted in an ultrahigh vacuum (UHV) chamber with a base pressure of less than 5×10^{-11} Torr. 4-*trans*-2-(pyrid-4-yl-vinyl) benzoic acid (PVBA) (Fig. 1) was synthesized and prepared for study in UHV by previously reported methods [17–21]. PVBA was evaporated from a Topac miniature Knudsen cell fitted with a Pt/Rh thermocouple, which allowed reproducible dosing as a function of time. The evaporation cell was located approximately 25 cm from the substrate surface and all depositions were performed along the surface normal with a substrate temperature of ~ 300 K. PVBA molecules were deposited at background pressures less than 1×10^{-10} Torr. The deposition rate and coverage were calibrated with STM at a range of evaporator temperatures. For the experiments presented here, a cell temperature of 128 °C was employed and enabled a deposition rate of ~ 0.1 monolayer (ML) per minute.

A single crystal Pd(1 1 1) surface (Matek, Julich, Germany) was employed for all of the studies presented here. The atomically flat Pd(1 1 1) surface was prepared by repeated cycles of argon sputtering ($5.5 \mu\text{A}/\text{cm}^2$, 1 keV), annealing in oxygen partial pressures of 5×10^{-10} Torr at 700 °C for 3 min, and subsequent vacuum-annealing at 1000 °C for 15 min. The cleanliness and crystallographic order were followed respectively with Auger electron spectroscopy (AES) and low energy electron diffraction (LEED) using an Omicron retarding field analyzer and LEED optics. The structures resulting from the adsorption of PVBA on Pd(1 1 1) were investigated at room temperature with an Omicron UHV AFM/STM LF1 head, in turn controlled by RHK STM 1000 electronics and software. In this arrangement, the sample was scanned with respect to a fixed tip (Pt) position. The STM measurements were performed in the constant current mode with a sample bias of -1.0 V and tunneling currents of 250 pA, i.e., in the high tunneling resistance regime (a gap resistance of ~ 4 G Ω). At gap resistances < 1 G Ω and tunneling currents > 1.0 nA, tip-induced motion of the adsorbate was frequently observed. Typical high resolution STM images of the clean substrate

revealed a well-ordered atomic lattice with defect densities less than 5%.

3. Results and discussion

The Pd(1 1 1) surface was prepared according to the procedures described above and imaged with STM in the low resistance tunneling mode at room temperature. Large area constant current images revealed terraces ~ 50 nm in width, separated by monoatomic steps 0.22 nm in height. Small area, constant current images clearly revealed the hexagonal structure of the (1 1 1) surface (data not shown). Although these features are not readily visible in the data presented below due to differences in the tunneling conditions, they served as a quantitative calibration point for both the dimensions and crystallographic orientation of the adsorbed structure.

Following this characterization, the surface was exposed at room temperature to PVBA. Although a range of exposures was studied, we focus in this paper on the low coverage regime and the role of substrate–adsorbate interactions in the formation of the observed structures. Fig. 2 displays the constant current image of a $20\text{ nm} \times 20\text{ nm}$ region following a ~ 0.1 ML dose. The image contains seventeen rod-like structures with varied orientation and one Y-shaped structure. The ‘size’ of the structures was characterized by taking cross-sections of the STM signal (calibrated piezo voltage) through the structures. The full-width half-height of the profile along the rod-like structures measured 3.4 ± 0.1 nm and is consistent with species composed of PVBA dimer pairs. The approximate size and shape of the molecular features of the monomer unit are consistent with those of PVBA imaged on other surfaces [17–21]. However, the overall length of the dimer structures suggests that the intermolecular forces responsible for the pairing have been slightly perturbed with respect to the periodicity of one-dimensional superstructures of PVBA on weakly interacting substrates. This perturbation of intermolecular forces is thought to originate from the relatively stronger adsorption interaction of PVBA on Pd(1 1 1). The Y-shaped structures were assigned as PVBA trimers through

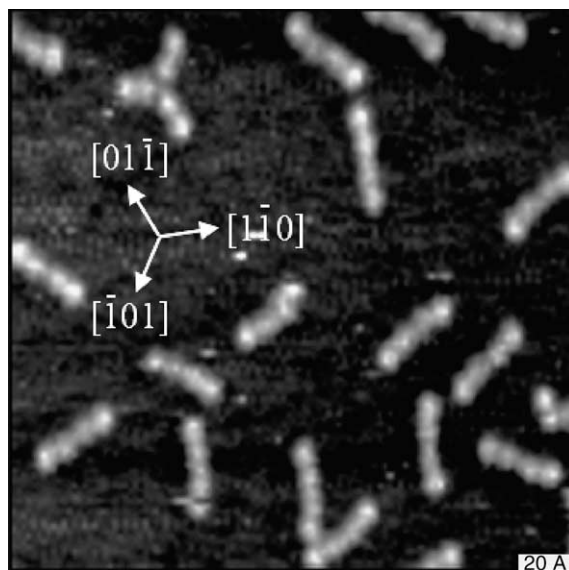


Fig. 2. Two different forms of self-assembled structures, dimers and trimers, were observed on Pd(1 1 1) at room temperature at a ~ 0.1 ML coverage ($200\text{ Å} \times 200\text{ Å}$). The dimers consist of two PVBA molecules, each of which appears with two lobes of intensity, while the trimers, appearing with less frequency, consist of three PVBA molecules.

a similar analysis and are thought to arise from intermolecular interactions involving three carboxylic acid moieties, or two carboxylic groups and one pyridyl group. Isolated monomers of PVBA and linear trimers were also observed in a very few number of instances; however the dimer structure was characteristic of $\sim 85\%$ of the observed structures ($\sim 85\%$ dimers, $\sim 13\%$ trimers and $\sim 2\%$ tetramers and hexamers for 454 clusters) and is the focus of our discussion in this report. These observations suggest that the deposited molecules are mobile upon adsorption and diffuse on the surface until an intermolecular interaction is formed. A cluster composed of two or more PVBA molecules is observed to be immobilized with respect to time scale of these measurements, consistent with an enhanced diffusion energy barrier of the cluster. This scenario is also consistent with the absence of larger aggregate structures and implies that the diffusion barrier of dimer and trimer structures is greater than thermal energy at room temperature.

Upon further examination of the dimers, two forms of dimer adsorption structures could be

noted in Fig. 2. Fig. 3a and c present high resolution images of the two types of dimers. A line bisecting the intensity maxima of the outer lobes is drawn to highlight the different geometries of the two structures. In Fig. 3a, the components of the dimer are related through a C_2 rotation and together produce a linear structure, while the dimer portrayed in Fig. 3c is composed of monomers related by reflection through a mirror plane and thus produce a bent structure. The formation of the different dimer structures is afforded through a surface-induced chirality of the PVBA molecule; adsorption on the planar surface produces two nonsuperimposable structures (δ and λ) (Fig. 1). Fig. 3b and d illustrate this effect by overlaying skeletal structures of PVBA on two-tone reductions of

the STM images presented in Fig. 3a and c. From these representations, it is clear that the difference in the dimer structures arises from the relative orientation of the vinyl linkages of the two PVBA monomers (Fig. 1).

Further evidence for the unique dimer structures is found in the analysis of their orientation relative to atomic rows of the Pd surface. The crystallographic axes shown in Figs. 2 and 3 have been determined from both corresponding LEED images and an FFT analysis of the STM images of the clean Pd(111) surface. While the dimer structures do not lie along atomic rows, they are oriented in specific directions. The homo-chiral dimers are observed to lie $\pm 20^\circ$ from one of three equivalent low index directions on the Pd(111)

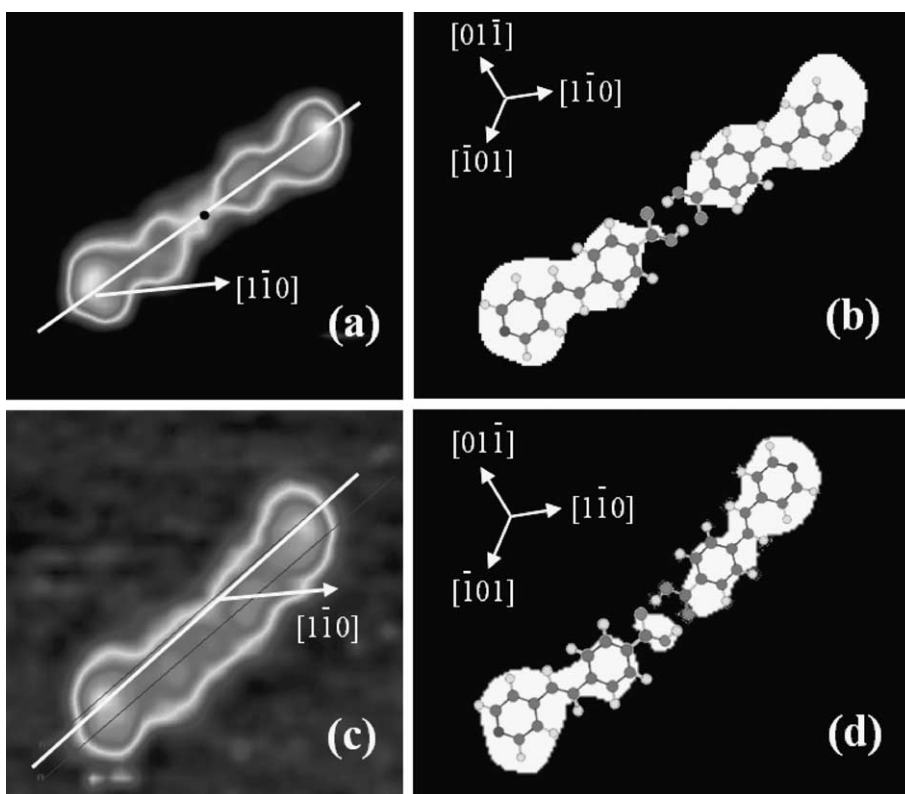


Fig. 3. (a) A high resolution image ($42 \text{ \AA} \times 42 \text{ \AA}$) of the straight dimer structure reveals the linear alignment of the two adsorbed PVBA monomers. (b) Scaled molecular structures overlay a two-tone reduction of the STM image in (a). The linear dimer is composed of two PVBA molecules with a “ δ ” orientation. (c) A high resolution image of the bent dimer illustrates that the two PVBA monomers do not share a common axis, indicating different adsorption orientations with respect to the Pd lattice. (d) Scaled molecular structures overlay the two-tone reduction of the STM image in (c). The bent dimer is composed to two PVBA monomers with opposite surface-induced chiralities.

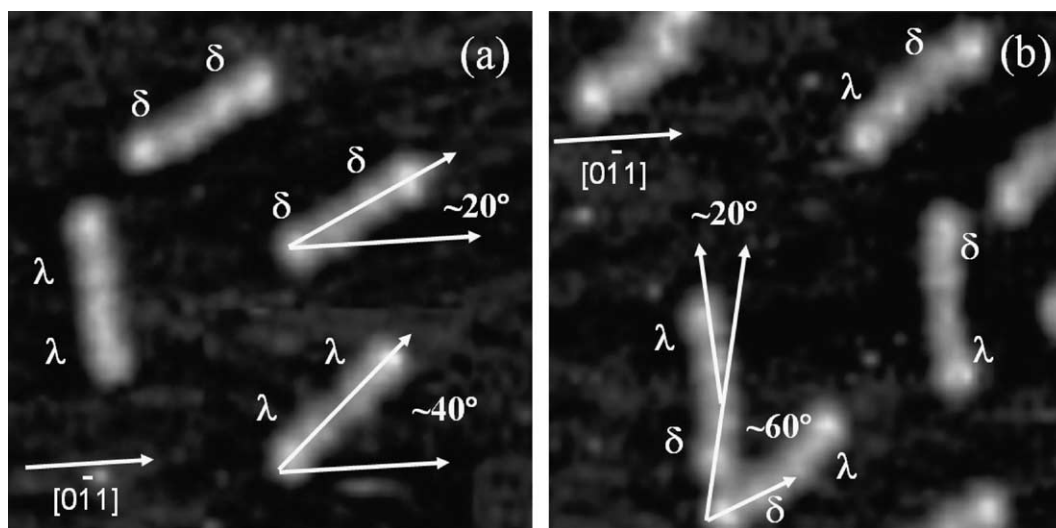


Fig. 4. Distinct orientations of the PVBA dimer structures were observed across the surface. Representative images of different regions of the surface ($100 \text{ \AA} \times 100 \text{ \AA}$) illustrate the range of structures observed. (a) Linear dimer structures were observed with their axis oriented $\pm 20^\circ$ from the low index directions on the Pd surface. Specific orientations could be assigned to the $\delta\delta$ and $\lambda\lambda$ dimers (see text). (b) The adsorption geometry of bent dimers, composed of δ and λ species, resulted from the relative orientation of the two different surface-induced chiral structures of PVBA.

surface ($[1\bar{1}0]$, $[10\bar{1}]$ and $[01\bar{1}]$) (Fig. 4a). Close inspection of the linear dimer structures with respect to the location of intensity maxima also allowed separation into the two possible types of homo-chiral structures ($\delta\delta$ and $\lambda\lambda$, Fig. 1, where the notation of their orientation has been adopted from a previous publication [17]). The six observed orientations of the linear dimer are consistent with a site specific adsorption of the $\delta\delta$ and $\lambda\lambda$ structures, with $\delta\delta$ structures being observed in three orientations $+20^\circ$ from the low index directions along the Pd surface and $\lambda\lambda$ structures being observed in three orientations -20° from the low index directions. This observation further explains the bent geometry of the hetero-chiral $\delta\lambda$ and $\lambda\delta$ dimer structures (Fig. 4b). Given the possible orientations of the individual δ and λ structures, the molecular axes of monomers in $\delta\lambda$ and $\lambda\delta$ structures will differ in orientation by multiples of 20° . The vast majority of hetero-chiral dimer structures were observed with a 20° angle between the orientations of the molecular axes. While these studies do not reveal the exact nature of the adsorption site(s), it is clear that local energy minima arise from cooperative interactions of the entire

PVBA dimer with the corrugated electronic structure of the Pd(111) surface. Although simultaneous imaging of the Pd lattice and PVBA molecules proved to be difficult, a qualitative model suggests such monomer orientations are consistent with an adsorption geometry that places the two ring structures of PVBA over threefold hollow sites. Additional measurements and calculations will be required to substantiate such a model.

The statistics of the relative appearance of the different dimer structures are presented in Fig. 5. In this assessment, individual monomers have been labeled as “ δ ” or “ λ ” (Fig. 1) based on the local orientation of the two aromatic ring structures in PVBA observed in the high resolution STM images. As previous studies [21] have concluded that the transfer of H from one oxygen to the other within the carboxylic acid moiety is facile, we assume that structural variations beyond those of Fig. 1 are not induced through adsorption. As before, surface-induced chirality results in the possibility of two homo-chiral linear dimers, $\delta\delta$ and $\lambda\lambda$, and two structurally equivalent hetero-chiral bent dimers, $\delta\lambda$ and $\lambda\delta$ (Fig. 5a and b). This

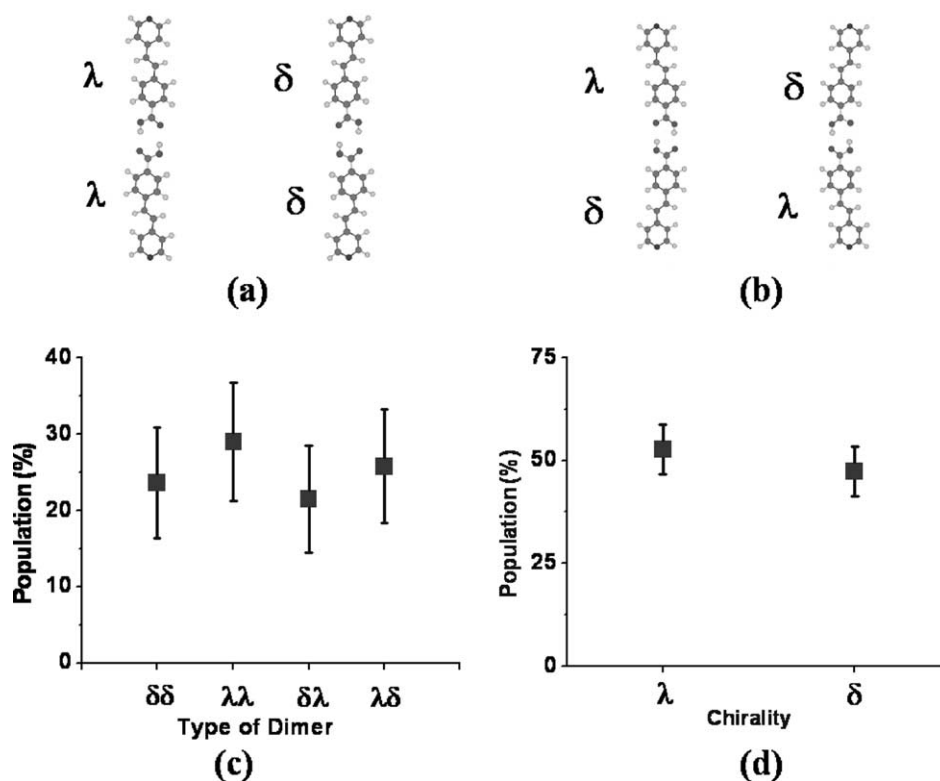


Fig. 5. A statistical analysis of PVBA dimer pairs (93 structures) assessed the presence of (a) two homo-chiral linear dimers and (b) two hetero-chiral bent dimers. (c) An equal abundance of each different structure was observed for this data set and indicates (d) a racemic mixture of the “ λ ” and “ δ ” PVBA adsorption structures on the Pd(1 1 1) surface.

notation scheme involves labeling structures on the surface in a left to right fashion. An assessment of 93 dimer structures has been carried out and indicates that statistically equivalent numbers of the four dimer species exist on the surface (Fig. 5c), consistent with an equal mixture of the “ δ ” and “ λ ” PVBA structures present on the Pd surface (Fig. 5d). The error bars in Fig. 5 refer to the statistical error with respect to sample size and are calculated as $165\sqrt{(p(1-p)/N)}$, where N is total number of samples and p is the sample size divided by N .

Previous investigations of the adsorption of PVBA on other fcc metals produced very different results with respect to the structure of the adsorbed species. On Pd(1 1 0), Weckesser et al. [17,18] observed isolated PVBA monomers having one of two distinct orientations with respect to the [1 $\bar{1}$ 0] direction. The appearance of two orienta-

tions was ascribed to the adsorption of the δ and λ structures of PVBA. In contrast, PVBA adsorption on Ag(1 1 1) and Au(1 1 1) led to the formation of long ($\sim\mu\text{m}$) one-dimensional double chains composed of a network of hydrogen-bonded PVBA monomers [19–21]. Intermolecular forces were observed to play a major role both along a single chain as the molecules aligned in a head to tail fashion as well as between the chain pairs [25,26]. In these studies, a high degree of chiral correlation was inferred within the domains of the one-dimensional chains, i.e., only a single chiral orientation of PVBA made up the supramolecular structure. (All previous STM studies of this system have been collected at cryogenic temperatures.)

The results described in this study of PVBA on Pd(1 1 1) represent an intermediate case to those of previous studies. On Pd(1 1 1), both intermolecular interactions (dimer and trimer pairing) and ad-

sorbate–substrate interactions (preferential orientation of dimer and trimer structures) play a significant role in the observed structures. The intermediate adsorbate–substrate interaction is entirely consistent with the expected trend in adsorption energies. In analogy, measurements of adsorption energies of benzene on these substrates shows that Pd(110) > Pd(111) > Ag(111), Au(111) [27–30]. While intermolecular attractions are inherently a function of the molecular details of interacting species, their influence on the resulting structures observed on Pd(111) differs from that observed on the other (111) surfaces where extended chains form through this mechanism. On Pd(111), we judge that the increased interaction between PVBA and the Pd(111) surface serves to interrupt the formation of larger supramolecular assemblies through the existence of lower energy adsorption sites that lead to increased intermolecular separations. An absolute assessment of hydrogen bonding distances and local head-to-tail orientations within the dimer structures was precluded in this study due to the absence of extended periodicity in the structures (as was observed in the chains on Ag(111) and Au(111)). Furthermore, room temperature STM imaging conditions limited the ultimate resolution of the molecular species. Nonetheless, we surmise that many of intermolecular interactions leading to the observed structures are comprised of head-to-head (carboxylic acid) as these represent the strongest possible interaction for dimers [20].

4. Conclusions

The adsorption of PVBA on Pd(111) at 300 K produces molecular dimers and trimers. The size and orientation of these molecular clusters is determined through a cooperative interplay between substrate and adsorbate interaction and intermolecular hydrogen bonding interactions. The exact nature of the adsorption structure is further defined by a surface-induced chirality of the approximately planar, asymmetric PVBA molecule. While a statistical analysis of the distribution of geometries reveals a racemic mixture of orientations on the surface, these studies clearly portray

the opportunities for design of self-assembled supramolecular structures through synthetic tailoring of molecules becoming chiral upon adsorption, and appropriate selection of substrate.

Acknowledgements

This work was supported by the Texas Higher Education Coordinating Board—Advanced Technology Program, grant no. 003652-0365-1999. BIK acknowledges fruitful discussions with Y. Na.

References

- [1] G.A. Attard, *J. Phys. Chem. B* 105 (2001) 3158.
- [2] J.D. Horvath, A.J. Gellman, *J. Am. Chem. Soc.* 124 (2002) 2384.
- [3] K.H. Ernst, M. Bohringer, C.F. McFadden, P. Hug, U. Müller, U. Ellerbeck, *Nanotechnology* 10 (1999) 355.
- [4] M. Schunack, E. Laegsgaard, I. Stensgaard, I. Johannsen, F. Besenbacher, *Angew. Chem. Int. Ed.* 40 (2001) 2623.
- [5] M. Schunack, F. Rosei, Y. Naitoh, P. Jiang, A. Gourdon, E. Laegsgaard, I. Stensgaard, C. Joachim, F. Besenbacher, *J. Chem. Phys.* 117 (2002) 6259.
- [6] M. Schünack, L. Petersen, A. Kühnle, E. Laegsgaard, I. Stensgaard, I. Johannsen, F. Besenbacher, *Phys. Rev. Lett.* 86 (2001) 456.
- [7] M.O. Lorenzo, C.J. Baddeley, C. Muryn, R. Raval, *Nature* 404 (2000) 376.
- [8] Q. Chen, D.J. Frankel, N.V. Richardson, *Surf. Sci.* 497 (2002) 37.
- [9] E.M. Marti, S.M. Barlow, S. Haq, R. Raval, *Surf. Sci.* 501 (2002) 191.
- [10] A. Kühnle, T.R. Linderth, B. Hammer, F. Besenbacher, *Nature* 415 (2002) 891.
- [11] R. Raval, *J. Phys.: Condes. Matter* 14 (2002) 4119.
- [12] M.O. Lorenzo, S. Haq, T. Bertrams, P. Murray, R. Raval, C.J. Baddeley, *J. Phys. Chem. B* 103 (1999) 10661.
- [13] Y.J. Zhang, M. Jin, R. Lu, Y.L. Song, L. Jiang, Y.Y. Zhao, T.J. Li, *J. Phys. Chem. B* 106 (2002) 1960.
- [14] M. Böhringer, W.D. Schneider, R. Berndt, *Angew. Chem. Int. Ed.* 39 (2000) 792.
- [15] M. Böhringer, K. Morgenstern, W.-D. Schneider, R. Berndt, F. Mauri, A. De Vita, R. Car, *Phys. Rev. Lett.* 83 (1999) 324.
- [16] G.P. Lopinski, D.J. Moffat, D.D.M. Wayner, R.A. Wolkow, *Nature* 392 (1998) 909.
- [17] J. Weckesser, J.V. Barth, C.Z. Cai, B. Müller, K. Kern, *Surf. Sci.* 431 (1999) 168.
- [18] J. Weckesser, J.V. Barth, K. Kern, *J. Chem. Phys.* 110 (1999) 5351.

- [19] J.V. Barth, J. Weckesser, C. Cai, P. Günter, L. Burgi, O. Jeandupeux, K. Kern, *Angew. Chem. Int. Ed.* 39 (2000) 1230.
- [20] J.V. Barth, J. Weckesser, G. Trimarchi, M. Vladimirova, A. De Vita, C.Z. Cai, H. Brune, P. Günter, K. Kern, *J. Am. Chem. Soc.* 124 (2002) 7991.
- [21] J. Weckesser, A. De Vita, J.V. Barth, C. Cai, K. Kern, *Phys. Rev. Lett.* 87 (9) (2001) 096101-1.
- [22] C. Cai, M.M. Bösch, B. Müller, Y. Tao, A. Kündig, C. Bösshard, Z. Gan, I. Biaggio, I. Liakata, M. Jäger, H. Schwer, P. Günter, *Adv. Mater.* 11 (1999) 745.
- [23] B. Müller, M. Jäger, Y. Tao, A. Kündig, C. Cai, C. Bösshard, P. Günter, *Opt. Mater.* 12 (2/3) (1999) 345–350.
- [24] C. Cai, M.M. Bösch, Y. Tao, B. Müller, Z. Gan, A. Kündig, C. Bösshard, I. Liakatas, M. Jaeger, P. Günter, *J. Am. Chem. Soc.* 120 (1998) 8563.
- [25] T. Yamamoto, H. Kokubo, *Mol. Cryst. Liquid Cryst.* 381 (2002) 113.
- [26] L.J. Prins, D.N. Reinhoudt, P. Timmerman, *Angew. Chem.-Int. Ed.* 40 (2001) 2383.
- [27] M. Fujisawa, T. Sekitani, Y. Morikawa, M. Nishijima, *J. Phys. Chem.* 95 (1991) 7415.
- [28] W.T. Tysoe, R.M. Ormerod, R.M. Lambert, G. Zgrablich, A. Ramires-Cuesta, *J. Phys. Chem.* 97 (1993) 3365.
- [29] M. Kakazawa, G. Somorjai, *Appl. Surf. Sci.* 68 (1993) 517.
- [30] X.-L. Zhou, M.E. Castro, J.M. White, *Surf. Sci.* 238 (1990) 215.